

# Unique Case of a Rare Mesenchymal Tumor Harboring a Somatic c.119delC *VHL* Mutation

Debbie G. Robbrecht, MD<sup>1</sup>; Florence Atrafi<sup>1</sup>; Job van Riet<sup>1</sup>; Ferry A.L.M. Eskens<sup>1</sup>; Paul J. van Diest<sup>2</sup>; Edwin P.J.G. Cuppen<sup>2</sup>; Geert J.L.H. van Leenders<sup>1</sup>; Harmen J.G. van de Werken<sup>1</sup>; and Martijn P. Lolkema<sup>1</sup>

## INTRODUCTION

The *VHL* gene is a tumor suppressor gene located at chromosome 3p25,<sup>1</sup> and its protein has multiple functions linked to multiple effector proteins.<sup>2</sup> Aberrations in the *VHL* gene are associated with sporadic clear cell renal cell carcinomas (ccRCCs), sporadic hemangioblastomas, pheochromocytomas, pancreatic islet cell tumors, endolymphatic sac tumors, and benign cysts affecting various organs.<sup>3</sup> Germline inactivation of the *VHL* gene causes the autosomal dominant von Hippel-Lindau (VHL) syndrome. *VHL* is rarely mutated outside of the context of RCC or VHL syndrome-associated malignancies.<sup>4</sup> Biallelic *VHL* inactivation caused by genetic and epigenetic alterations (including DNA methylation, histone modifications, and coincidental loss of genes localized adjacent to the *VHL* chromosome locus) has been described.<sup>2</sup> In both hereditary and sporadic tumors, *VHL* mutations are heterogeneous.<sup>5</sup>

The encoded VHL protein (pVHL) plays an important role in ubiquitination and proteosomal degradation of hypoxia inducible factor-1  $\alpha$  (HIF-1 $\alpha$ ). HIF-1 $\alpha$  activates transcription of genes (ie, target genes related to adaptation to hypoxia, such as vascular endothelial growth factor [VEGF] and platelet-derived growth factor  $\beta$  [PDGF $\beta$ ])<sup>6-8</sup> and acts in cellular processes such as metabolism, cellular senescence, chemotaxis, proliferation, transcription, WNT signaling, ubiquitinating RNA polymerase, and regulating nuclear factor  $\kappa\beta$ .<sup>2</sup> Here, we present a case report of a patient with metastasized follicular dendritic cell sarcoma (FDCS) harboring a somatic c.119delC *VHL* mutation. Our aim was to investigate the (epi)genetic background of this patient's disease and to determine whether the identified *VHL* mutation could be a driving mutation in this patient's FDCS.

## METHODS

### Case Report

In 2013, a 29-year-old female patient presented with a large abdominally located mass and multiple hepatic lesions. A histologic biopsy from a liver lesion showed an epithelioid and spindle cell malignant neoplasm with scattered lymphocytes. Immunohistochemistry (IHC) results matched the pattern of FDCS with expression of follicular dendritic cell markers CD21,

CD23, and CD35<sup>9</sup> (Fig 1A-C). Ewing sarcoma breakpoint region 1 (ESWR 1) was not detected with fluorescence in situ hybridization. On the basis of radiologic diagnosis, the pattern did not fit an RCC. This was further supported by a negative paired box gene 8 (PAX8) IHC result (Fig 1D).

The clinical course of our patient's disease is outlined in Figure 2. The first-line treatment consisted of eight cycles of CHOP (cyclophosphamide, doxorubicin, vincristine, prednisone), resulting in a metabolic complete response. Approximately 8 months later, progressive disease was apparent, with fluorodeoxyglucose-positive lymph nodes in the hepatic hilum (Fig 3A and 3B). The second-line treatment was pazopanib, which resulted in unexpected stable disease for 22 months.

The patient participated in the Dutch National Center for Personalized Cancer Treatment (CPCT)-02 program,<sup>10</sup> rendering additional tumor sampling for whole-genome sequencing (WGS) analysis before and after treatment with pazopanib. DNA was extracted from fresh-frozen biopsies obtained from a hepatic metastatic lesion and blood as a germline control. WGS was performed on the Illumina HiSeq X platform with 100 ng DNA as input using standard protocols (paired-end 2  $\times$  150 base pairs; Illumina, San Diego, CA). Within the framework of CPCT-02, all germline variants are filtered, which guarantees that only somatic variants are reported. Tumor samples and control blood were sequenced with a minimum base coverage depth of 90 $\times$  and 30 $\times$ , respectively. Somatic single nucleotide and indel variant calling was performed by an optimized bioinformatics pipeline (<https://github.com/hartwigmedical/>) on the basis of Strelka2 (v1.0.14-1).<sup>11</sup> Additional filtering against a panel of nearly 2,000 control genomes removed variants that were present in six or more of these respective samples. Germline and somatic structural variant detection was performed using Illumina Manta (v.1.0.3) and were post-processed using a custom application (Break Point Inspector; <https://github.com/hartwigmedical/>) to filter false-positive candidates and to discover exact breakpoint positions.<sup>12</sup> In both biopsies, WGS showed a somatic c.119delC *VHL* mutation, which prompted us to identify the meaning and importance of this variant in our patient.

Author affiliations and support information (if applicable) appear at the end of this article.

Accepted on September 18, 2018 and published at [ascopubs.org/journal/po](https://ascopubs.org/journal/po) on February 6, 2019; DOI <https://doi.org/10.1200/P0.18.00244>

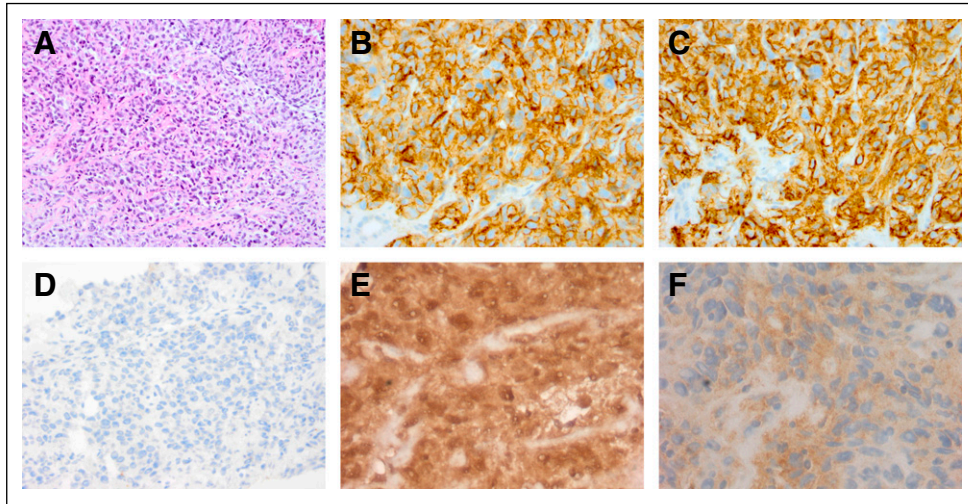


**FIG 1.** Immunohistochemistry (IHC). The liver biopsy showed large solid fields of discohesive epithelioid and spindle cells with basophilic cytoplasm, round to oval nucleus, and moderately enlarged nucleoli. A moderate number of scattered lymphocytes was present throughout the lesion. The cells were moderately pleomorphic with frequent mitoses. Hematoxylin and eosin immunohistochemistry (HE IH)  $\times 100$  (A). The tumor cells were strongly positive for CD21 (B), CD23 (C), and SMA; CD35 was locally positive. Calretinin, CD20, CD117, chromogranin, desmin, DOG1, EMA, KERAN, KL1, Melan A, S100, and synaptophysin were negative. Paired box gene 8 (PAX8) IHC was negative (D). HIF-1 $\alpha$  IHC showed positive nuclear staining (E), and glucose transporter 1 (GLUT1) IHC showed positive staining (F).

## RESULTS

### Genomic Landscape

The identified c.119delC *VHL* frameshift mutation led to a truncated pVHL (p.Pro40fs; Fig 4). Both biopsies showed genome-wide aberrations, with large chromosomal copy number alterations, structural rearrangements, and mutations in a broad spectrum of loci (Fig 5). Amplification of the *VHL* locus 3p25 was identified in both biopsies, with germline-informative B-allele frequencies revealing loss of heterozygosity. This finding hints toward a model in which the remaining *VHL* allele had been duplicated (and subsequently mutated), resulting in three *VHL* loci in biopsy 1

(two *VHL*<sub>WT</sub> and one *VHL*<sub>c.119delC</sub>) and seven *VHL* loci in biopsy 2 (two *VHL*<sub>WT</sub> and five *VHL*<sub>c.119delC</sub>). Identified variants and translocations differed between biopsies 1 and 2, with a remarkable reduction in translocations in the post-treatment biopsy (Fig 5).

### Consequences of the Identified c.119delC *VHL* Mutation

The primary question about the identified *VHL* mutation concerned the functional consequence at the protein level and whether this variation could be a driver mutation. Overproduction of HIF-1 $\alpha$  in the absence of hypoxia is the main effect of pVHL functional loss.<sup>13</sup> Therefore, we performed IHC on the second biopsy for HIF-1 $\alpha$  (Fig 1E),

Treatment	T0	Eight Cycles of CHOP	T6	No Treatment	T14*	Pazopanib	T36*	Phase 1 Trial	T47
Response			Metabolic CR		PD	SD	PD	SD	PD

**FIG 2.** Clinical course of the disease. The patient was diagnosed with follicular dendritic cell sarcoma in November 2013 (T0). The patient received eight cycles of CHOP (cyclophosphamide, doxorubicin, vincristine, prednisone), which resulted 6 months later (T6) in metabolic complete remission (CR). Eight months later (T14), the patient had progressive disease (PD). At T14, she was treated with pazopanib. In response to pazopanib, the patient had stable disease (SD) for a total of 22 months. After that (T36), the patient showed PD and participated in a phase 1 trial with immunotherapy (CD40 agonistic monoclonal antibody) in combination with vanucizumab (anti-angiopoietin-2 and anti-VEGF [vascular endothelial growth factor]) for 11 months. (\*) Tumor biopsies were obtained before the start of treatment with pazopanib and after its discontinuation.

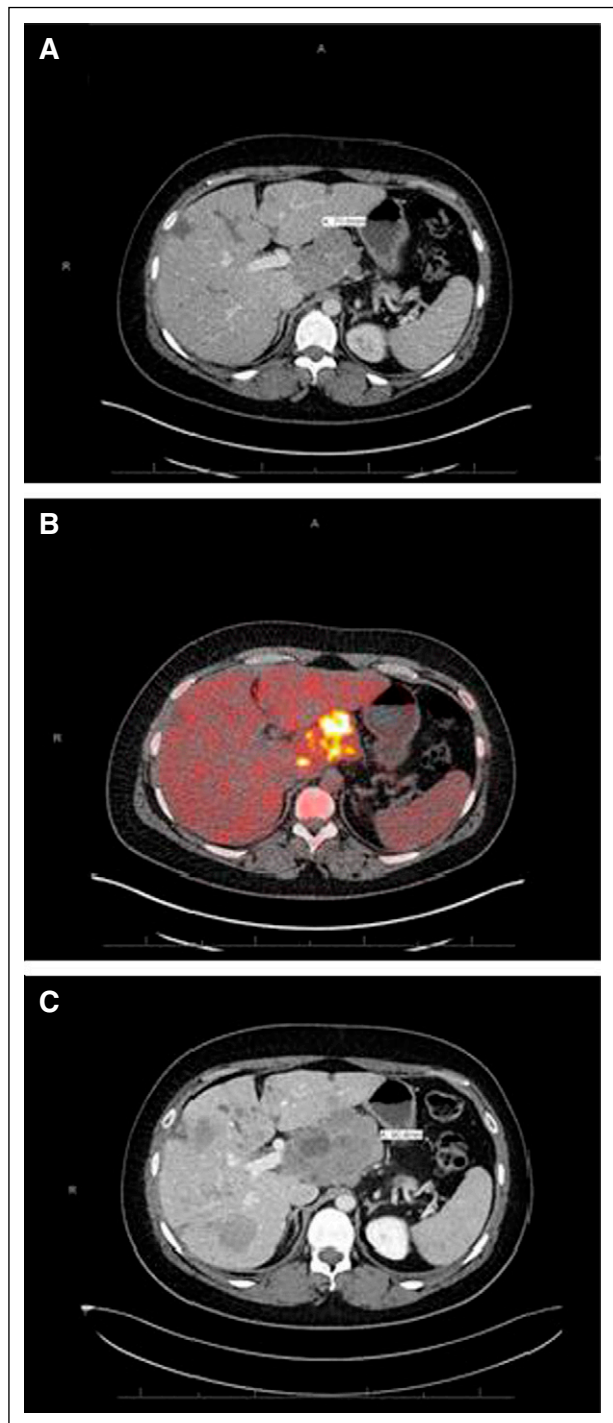


**FIG 3.** Localization and progression of our patient's follicular dendritic cell sarcoma. In March 2016, progressive disease was revealed on a conventional CT scan (A) and on a positron emission tomography scan (B) before the start of treatment with pazopanib. In January 2017, progressive disease persisted after 22 months of treatment with pazopanib (C).

which showed positive nuclear staining, and for glucose transporter 1 (GLUT1; a glucose transporter associated with HIF-1 $\alpha$  downstream activation), which showed positive

staining (Fig 1F). Both results provide circumstantial evidence for functional loss of pVHL.<sup>7,10</sup>

## DISCUSSION

Our analysis revealed a unique patient with FDCC harboring a somatic functional *VHL* aberration, which is the first description of a *VHL* mutation in sarcoma.<sup>14</sup> Because FDCC is a rare mesenchymal neoplasm with a largely unknown and rather complex genetic landscape<sup>15</sup> and is unknown for harboring *VHL* aberrations, we verified specific IHC-based markers to confirm the diagnosis and to reject metastatic RCC (mRCC) as an alternative diagnosis. The positive HIF-1 $\alpha$  IHC result may indicate a functional loss of pVHL; in this patient, it was a consequence of mutation and potential methylation-derived changes leading to biallelic *VHL* gene inactivation. Although most evidence in FDCC has been found for the involvement of the RAS/RAF signaling pathway,<sup>16,17</sup> we did not identify mitogen-activated protein kinase (MAPK) alterations in our patient. All evidence collected points toward FDCC with a functional *VHL* mutation. A mutant allele-specific imbalance as a consequence of allele-specific amplification has been described.<sup>18,19</sup> However, this seems to be a more common aspect with activating mutations. Recurrent *VHL* locus amplifications have not been described in ccRCC; therefore, it does not seem to be a common aberration. However, these reports did not specifically investigate post-tyrosine kinase samples.<sup>2,20,21</sup>

Numerous nonspecific chromosomal translocations were present in the pretreatment biopsy, with a remarkable decline in the number of structural variants (SVs) following treatment with pazopanib. Treatment of cancer may have an influence on involved processes and subsequently on patterns and frequency of SVs.<sup>22</sup> Alterations in the number of SVs between time points in a patient's malignancy may also be a consequence of tumor evolution and selective survival of subclonal populations as a result of the selective pressure of treatment, similar to variable somatic alterations that cause the emergence of drug resistance.<sup>23</sup> The changes in the genomic landscape between the two biopsies obtained in our patient could be associated with the observed disease response during treatment with pazopanib.<sup>24</sup> Moreover, the fact that the mutated *VHL* gene has been amplified in our patient's disease over time emphasizes its importance and potential as a driver mutation.

Upregulated VEGF is associated with the HIF pathway. In ccRCC, it is well known that HIF-1 $\alpha$  is constitutively activated by inactivation of the *VHL* gene. Pazopanib, a multikinase inhibitor with activity against the VEGF receptor and platelet-derived growth factor  $\alpha$  and  $\beta$  receptors, is effective in the treatment of mRCC<sup>25</sup> and metastatic sarcoma.<sup>26</sup> During treatment with pazopanib, our patient had stable disease for 22 months. The length of this progression-free survival (PFS) is significantly longer than

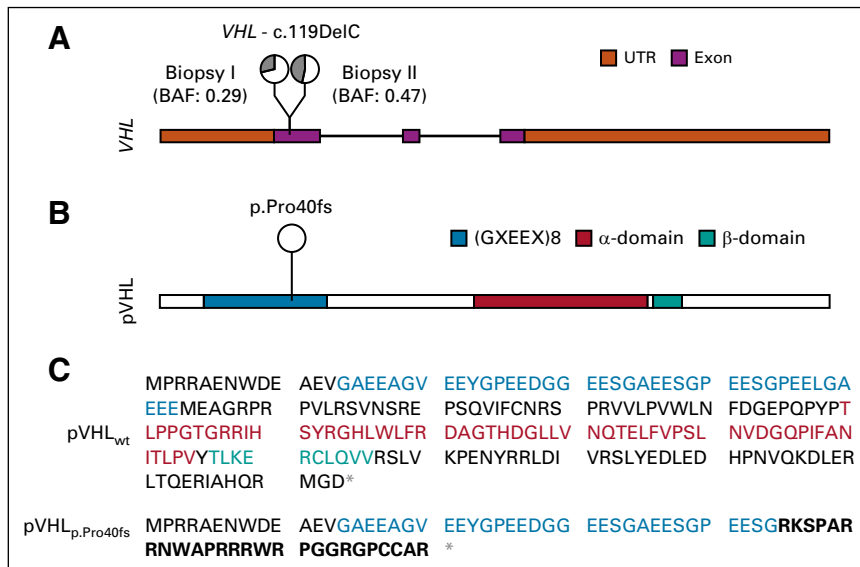


**FIG 4.** Change-of-function von Hippel Lindau (*VHL*) frameshift mutation (c.119delC) leads to truncated VHL protein (pVHL). (A) c.119delC mutation on a schematic model of premRNA *VHL* transcript with allelic frequencies of reference (GC) and alternative (G-) observations, colored white and gray, respectively. Untranslated regions (UTR) and exonic regions are depicted by rectangular boxes (colored dark blue and dark gold, respectively), and intronic regions are depicted by black lines. (B) c.119delC mutation on a schematic model of pVHL with predicted protein domains; (GXEE)8 is shown in violet,  $\alpha$ -domain in purple, and  $\beta$ -domain in pink. (C) Protein sequences of wild-type (wt) pVHL and mutant pVHL, colored by protein domains; (GXEE)8 is shown in light blue,  $\alpha$ -domain in light gold, and  $\beta$ -domain in red. (The *VHL* gene model is on the basis of Ensembl transcript NM\_000551.2 and the protein model is on the basis of the UniProtKB P40337 entry.) Red asterisk indicates stop codon. Bold text represents (predicted) aberrant sequence of amino acids (out-of-frame). BAF, B-allele frequencies.

the observed median PFS in the PALETTE trial<sup>26</sup> (4.6 months; 95% CI, 3.7 to 4.8 months). Moreover, Saygin et al<sup>27</sup> performed a pooled analysis of data from 462 patients with FDCC, showing a median survival for patients with metastatic disease of 9 months (range, 0.25 to 72 months) and a 2-year survival rate of 15.8%; these results suggest that the long PFS is not the result of better prognostic features of FDCC. The relatively long PFS during our patient's last treatment, which consisted of the combination of a CD40 agonistic monoclonal antibody and an anti-angiopoietin-2 and anti-VEGF bispecific monoclonal antibody, could possibly be explained by the effect of the latter drug (vanucizumab). These data imply that the *VHL* mutation in our patient may predict a biologic behavior more similar to mRCC than to a metastatic sarcoma in response to treatment with pazopanib. These findings are not sufficient to make an argument for VEGF-targeted therapies in

FDCC, because this is the first case of a *VHL*-mutated FDCC as far as we know.

Although HIF stabilization and GLUT1 accumulation are, at the most, indirect evidence for pVHL functional loss, a limitation of this case report is the absence of methylation analysis looking further into epigenetic silencing of the *VHL* gene. This is a consequence of the lack of normal control material from our patient, which made it impossible to correctly interpret the methylation analysis. In addition, there was no remaining material from biopsy 1 to perform additional IHC analysis.

In conclusion, this case report describes a patient with FDCC harboring a unique somatic mutation in *VHL*. This case underscores the scientific value of next-generation sequencing of a patient's genetic material to unravel the genomic profile of cancers and to identify potential genetic abnormalities that can be targeted by cancer therapies.

## AFFILIATIONS

<sup>1</sup>Erasmus University Medical Center, Rotterdam, the Netherlands

<sup>2</sup>University Medical Center Utrecht, Utrecht, the Netherlands

## CORRESPONDING AUTHOR

Debbie G. Robbrecht, Department of Medical Oncology, Erasmus MC Cancer Institute, Internal Oncology NT-5, Dr Molenwaterplein 40, 3015 GD, Rotterdam, Netherlands; e-mail: d.robbecht@erasmusmc.nl

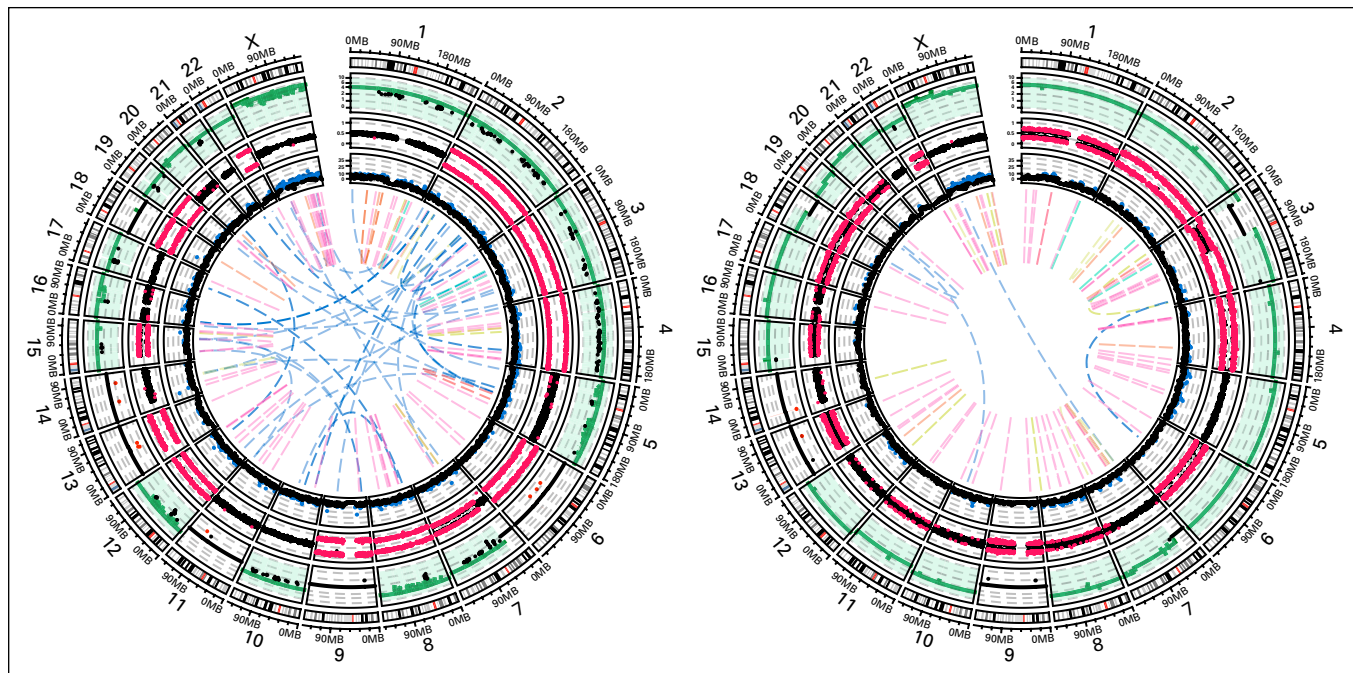


**FIG 5.** Genomic landscapes before and after treatment. (A) Biopsy obtained before pazopanib treatment. (B) Biopsy obtained after pazopanib treatment. The outermost track displays the ideogram of the human genome with exclusion of chromosome Y. The second outermost track displays absolute copy number estimations from zero copies to 10 copies. Regions with copy number gains (more than three copies; green) and copy number losses (zero copies; red). The third track displays the B-allele frequencies (BAFs) in the tumor(s) with germline-informative (heterozygous) markers. Regions displaying loss of heterozygosity ( $BAF \geq 0.66$  or  $\leq 0.33$ ) are colored in dark pink. The fourth outermost track displays the mutational burden per 1 Mb sliding windows. Higher numbers, indicated in blue, represent regions with more mutations. The innermost lines represent structural variations colored per type; interchromosomal translocations are shown in blue, deletions in pink, insertions in green-cyan, inversions in yellow-brown, and tandem duplications in brown.

#### AUTHOR CONTRIBUTIONS

**Conception and design:** Debbie G. Robbrecht, Florence Atrafi, Ferry A.L.M. Eskens, Martijn P. Lolkema

**Provision of study material or patients:** Ferry A.L.M. Eskens, Geert J.L.H. van Leenders, Martijn P. Lolkema

**Collection and assembly of data:** Debbie G. Robbrecht, Florence Atrafi, Job van Riet, Paul J. van Diest, Geert J.L.H. van Leenders, Martijn P. Lolkema

**Data analysis and interpretation:** Debbie G. Robbrecht, Florence Atrafi, Job van Riet, Paul J. van Diest, Edwin P.J.G. Cuppen, Harmen J.G. van de Werken, Martijn P. Lolkema

**Manuscript writing:** All authors

**Final approval of manuscript:** All authors

#### AUTHORS' DISCLOSURES OF POTENTIAL CONFLICTS OF INTEREST

The following represents disclosure information provided by authors of this manuscript. All relationships are considered compensated.

Relationships are self-held unless noted. I = Immediate Family Member, Inst = My Institution. Relationships may not relate to the subject matter of this manuscript. For more information about ASCO's conflict of interest policy, please refer to [www.asco.org/rwc](http://www.asco.org/rwc) or [ascopubs.org/po/author-center](http://ascopubs.org/po/author-center).

#### Florence Atrafi

**Travel, Accommodations, Expenses:** AbbVie, Astellas Pharma

#### Paul J. van Diest

**Consulting or Advisory Role:** Panterhei (Inst)

**Patents, Royalties, Other Intellectual Property:** DDX3 as a biomarker for cancer and methods related thereto (Inst)

#### Geert J.L.H. van Leenders

**Consulting or Advisory Role:** Roche

**Speakers' Bureau:** Roche

**Research Funding:** Roche (Inst), AstraZeneca (Inst)

#### Martijn P. Lolkema

**Consulting or Advisory Role:** Johnson & Johnson, Sanofi, Incyte, Novartis

**Research Funding:** Astellas Pharma (Inst), Sanofi (Inst), Johnson & Johnson (Inst), Merck Sharp & Dohme (Inst)

**Travel, Accommodations, Expenses:** Astellas Pharma, Merck Sharp & Dohme

No other potential conflicts of interest were reported.

#### ACKNOWLEDGMENT

We thank L. Looijenga and his team from the Department of Molecular Pathology. We thank Hartwig Medical Foundation for providing whole-genome sequencing data and for performing analysis of these data. Moreover, this patient was entered into the Center for Personalized Cancer Treatment (CPCT)-02 study. We acknowledge the contribution of the CPCT for enabling biopsies in this study to obtain genomic analyses.

## REFERENCES

1. Latif F, Tory K, Gnara J, et al: Identification of the von Hippel-Lindau disease tumor suppressor gene. *Science* 260:1317-1320, 1993
2. Mehdi A, Riazalhosseini Y: Epigenome aberrations: Emerging driving factors of the clear cell renal cell carcinoma. *Int J Mol Sci* 18:E1774, 2017
3. Maher ER, Kaelin WG Jr: von Hippel-Lindau disease. *Medicine (Baltimore)* 76:381-391, 1997
4. Lawrence MS, Stojanov P, Mermel CH, et al: Discovery and saturation analysis of cancer genes across 21 tumour types. *Nature* 505:495-501, 2014
5. Kim WY, Kaelin WG: Role of VHL gene mutation in human cancer. *J Clin Oncol* 22:4991-5004, 2004
6. Kaelin WG Jr: Molecular basis of the VHL hereditary cancer syndrome. *Nat Rev Cancer* 2:673-682, 2002
7. Frew IJ, Moch H: A clearer view of the molecular complexity of clear cell renal cell carcinoma. *Annu Rev Pathol* 10:263-289, 2015
8. Greijer AE, van der Groep P, Kemming D, et al: Up-regulation of gene expression by hypoxia is mediated predominantly by hypoxia-inducible factor 1 (HIF-1). *J Pathol* 206:291-304, 2005
9. Lymphoproliferative disorders associated with immune deficiencies and histiocytic and dendritic cell neoplasms, in Wahed A and Dasgupta A: *Hematology and Coagulation: A Comprehensive Review for Board Preparation, Certification and Clinical Practice*. Amsterdam, Netherlands, Elsevier, 2015, pp 225-30
10. Center for Personalized Cancer Treatment: Development of a platform for next-generation DNA sequencing based personalized treatment for cancer patients: Protocol to obtain biopsies from patients with locally advanced or metastatic cancer (CPCT - 02 biopsy protocol). [https://www.cpct.nl/wp-content/uploads/2017/04/CPCT-02\\_prot\\_am-8.0\\_v15\\_08-12-2016\\_Clean.pdf](https://www.cpct.nl/wp-content/uploads/2017/04/CPCT-02_prot_am-8.0_v15_08-12-2016_Clean.pdf)
11. Kim S, Scheffler K, Halpern AL, et al: Strelka2: Fast and accurate calling of germline and somatic variants. *Nat Methods* 15:591-594, 2018
12. Chen X, Schulz-Trieglaff O, Shaw R, et al: Manta: Rapid detection of structural variants and indels for germline and cancer sequencing applications. *Bioinformatics* 32:1220-1222, 2016
13. Iliopoulos O, Levy AP, Jiang C, et al: Negative regulation of hypoxia-inducible genes by the von Hippel-Lindau protein. *Proc Natl Acad Sci USA* 93:10595-10599, 1996
14. The Cancer Genome Atlas: TCGA data portal. <https://tcga-data.nci.nih.gov/docs/publications/tcga/>
15. Andersen EF, Paxton CN, O'Malley DP, et al: Genomic analysis of follicular dendritic cell sarcoma by molecular inversion probe array reveals tumor suppressor-driven biology. *Mod Pathol* 30:1321-1334, 2017
16. Wu A, Pullarkat S: Follicular dendritic cell sarcoma. *Arch Pathol Lab Med* 140:186-190, 2016
17. Go H, Jeon YK, Huh J, et al: Frequent detection of BRAF(V600E) mutations in histiocytic and dendritic cell neoplasms. *Histopathology* 65:261-272, 2014
18. Soh J, Okumura N, Lockwood WW, et al: Oncogene mutations, copy number gains and mutant allele specific imbalance (MASI) frequently occur together in tumor cells. *PLoS One* 4:e7464, 2009
19. LaFramboise T, Weir BA, Zhao X, et al: Allele-specific amplification in cancer revealed by SNP array analysis. *PLOS Comput Biol* 1:e65, 2005
20. Scelo G, Riazalhosseini Y, Greger L, et al: Variation in genomic landscape of clear cell renal cell carcinoma across Europe. *Nat Commun* 5:5135, 2014
21. Beroukhi R, Brunet JP, Di Napoli A, et al: Patterns of gene expression and copy-number alterations in von-Hippel Lindau disease-associated and sporadic clear cell carcinoma of the kidney. *Cancer Res* 69:4674-4681, 2009
22. Chiarle R: Translocations in normal B cells and cancers: Insights from new technical approaches, in Alt FW (ed): *Advances in Immunology*, Volume 117. Amsterdam, Netherlands, Elsevier, 2013, pp 39-71
23. Van Allen EM, Wagle N, Stojanov P, et al: Whole-exome sequencing and clinical interpretation of formalin-fixed, paraffin-embedded tumor samples to guide precision cancer medicine. *Nat Med* 20:682-688, 2014
24. Borad MJ, Champion MD, Egan JB, et al: Integrated genomic characterization reveals novel, therapeutically relevant drug targets in FGFR and EGFR pathways in sporadic intrahepatic cholangiocarcinoma. *PLoS Genet* 10:e1004135, 2014
25. Baldewijns MM, van Vlodrop IJ, Vermeulen PB, et al: VHL and HIF signalling in renal cell carcinogenesis. *J Pathol* 221:125-138, 2010
26. van der Graaf WT, Blay JY, Chawla SP, et al: Pazopanib for metastatic soft-tissue sarcoma (PALETTE): A randomised, double-blind, placebo-controlled phase 3 trial. *Lancet* 379:1879-1886, 2012
27. Saygin C, Uzunaslan D, Ozguroglu M, et al: Dendritic cell sarcoma: A pooled analysis including 462 cases with presentation of our case series. *Crit Rev Oncol Hematol* 88:253-271, 2013

